HTD-Vol. 221, Heat Pipes and Thermosyphons
ASME 1992

AN ANALYTICAL MODEL FOR THE DESIGN OF WICKLESS HEAT-PIPE HEAT EXCHANGERS

Alfonso Niro
Dipartimento di Energetica
Politecnico di Milano
Milan, Italy

Gian Paolo Beretta
Dipartimento di Ingegneria Meccanica
Università di Brescia
Brescia, Italy

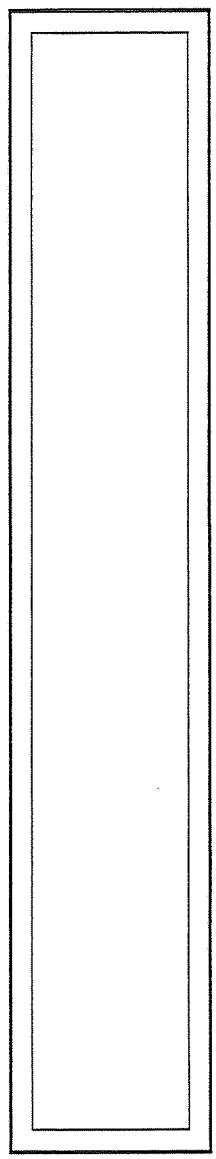

HTD-Vol. 221

HEAT PIPES
AND
THERMOSYPHONS

presented at
THE WINTER ANNUAL MEETING OF
THE AMERICAN SOCIETY OF MECHANICAL ENGINEERS
ANAHEIM, CALIFORNIA
NOVEMBER 8–13, 1992

sponsored by
THE HEAT TRANSFER DIVISION, ASME

edited by
W. S. CHANG
WRIGHT LABORATORY

F. M. GERNER
UNIVERSITY OF CINCINNATI

T. S. RAVIGURURAJAN
WICHITA STATE UNIVERSITY

THE AMERICAN SOCIETY OF MECHANICAL ENGINEERS
United Engineering Center ○□○□○ 345 East 47th Street ○□○□○ New York, N.Y. 10017

HTD-Vol. 221, Heat Pipes and Thermosyphons
ASME 1992

AN ANALYTICAL MODEL FOR THE DESIGN OF WICKLESS HEAT-PIPE HEAT EXCHANGERS

Alfonso Niro
Dipartimento di Energetica
Politecnico di Milano
Milan, Italy

Gian Paolo Beretta
Dipartimento di Ingegneria Meccanica
Università di Brescia
Brescia, Italy

In this paper, we present an analytical model to evaluate the thermal performance and the pressure drops of a gas-gas heat exchanger using wickless heat pipes, i.e., closed two-phase thermosyphons. We review the correlations to estimate the heat transfer coefficients both outside and inside thermosyphons, and the gas pressure drops through the exchanger. We derive an analytical correlation to evaluate the gas inlet temperatures to a tube-row as a function of row effectivenesses and heat capacity rates. We correlate the row effectiveness to the exchanger effectiveness. Finally, we analyze numerically the performances of a thermosyphon heat exchanger as predicted by the model for a low-temperature waste-heat application.

NOMENCLATURE

a	transverse pitch (interaxis distance between tubes in a row)
A_j	total surface area
A_{F_j}	finned surface area
A_{P_j}	thermosyphon evaporator or condenser surface area
A_{0_j}	unfinned pipe surface area ($= A_j - A_{F_j}$)
b	longitudinal pitch (distance between rows)
$C_{j,k}$	heat capacity rate
C_k^*	ratio of the hot to cold gas heat capacity rate ($= C_{2,k}/C_{1,k}$)
D	tube outer diameter
E	fin efficiency defined
$h_{out_{j,k}}$	average heat transfer coefficient outside thermosyphons
h_F	fin height
$h_{in_{j,k}}$	average heat transfer coefficient inside thermosyphons
K_P	thermal conductivity of the tube wall
N	rows of tubes
p_k	thermosyphon operating pressure
$\dot{q}_{Pk}$	heat transfer rate per thermosyphon
s	distance between the fins
T_{g_k}	thermosyphon operating temperature
$T_{1,k}$	hot gas outlet temperature to row k
$T_{1,k-1}$	hot gas inlet temperature to row k
$T_{2,k}$	cold gas inlet temperature to row k
$T_{2,k-1}$	cold gas outlet temperatures to row k
$U_{j,k}$	overall heat transfer coefficient defined by Equation 6
δ_P	tube wall thickness
ε_k	effectiveness of tube row kdefined by Equation 1
$\omega_{j,k}$	side effectiveness of tube row kdefined by Equations 2

INTRODUCTION

A heat-pipe heat exchanger is a parallel- or counter-flow exchanger. From the outside, it is quite similar to a finned-tube cross-flow exchanger, with the major difference being that the tubes are heat pipes. The bank of finned heat pipes is divided in the evaporator and condenser zones. The hot and cold gases flow separately across the evaporator and condenser zone, respectively. Also, since the exchanger has several rows of heat pipes (typically from 4 to 10), it may be considered a multipass exchanger. The rows of heat pipes may be aligned or staggered in the gas-flow direction. If the heat pipes are gravity-assisted, i.e., if they are closed two-phase thermosyphons called also wickless heat pipes, they must be operated vertically with the evaporator beneath the condenser; in this case, the exchanger operates in a superposed-

flow arrangement. A thermosyphon heat exchanger, being a reliable low-cost component with good performance, may be an appealing solution for low-temperature waste-heat recovery applications. Indeed, such applications are economically feasible only if the heat exchanger cost is very low, even at expense of thermal efficiency.

To analyze the thermal performance of a heat-pipe heat exchanger, the designer needs to correlate the effectiveness of the exchanger to that of each tube-row and, therefore, to the heat transfer characteristics both inside and outside the heat pipes. However, the models proposed in literature do not consider all of these aspects.

In this paper, we review the correlations to estimate the heat transfer coefficients both outside and inside thermosyphons, and the gas pressure drops through the exchanger. We derive an analytical correlation to evaluate the gas inlet temperatures to a tube-row as a function of row effectivenesses and heat capacity rates. We correlate the row effectiveness to the exchanger effectiveness. Finally, we analyze numerically the thermal performances and the pressure drops of a thermosyphon heat exchanger for a low-temperature application.

ANALYSIS

Consider a counterflow heat-pipe heat exchanger with N rows of tubes. Assume that inlet temperatures to the exchanger are uniform in the directions transverse to the flow, and that the heat pipes operate almost isothermally, so taht the temperature field inside the heat exchanger is one-dimensional. The effectiveness of the tube-row k is

$$\varepsilon_k = \frac{T_{2,k-1} - T_{2,k}}{T_{1,k-1} - T_{2,k}} \tag{1}$$

where $T_{2,k}$ and $T_{2,k-1}$ are, respectively, the cold gas inlet and outlet temperatures to row k, and $T_{1,k-1}$ is the hot gas inlet temperature to the same row. Since all the heat pipes in a row operate at the same temperature, for the tube row k we may define the evaporator-side and condenser-side effectiveness as

$$\omega_{1,k} = \frac{T_{1,k-1} - T_{1,k}}{T_{1,k-1} - T_{g_k}} \tag{2'}$$

$$\omega_{2,k} = \frac{T_{2,k-1} - T_{2,k}}{T_{g_k} - T_{2,k}} \tag{2"}$$

where T_{g_k} is the operating temperature of heat pipes in the row k.

If the heat exchanger operates in a steady-state and gases may be considered to behave as ideal gases, from an energy balance for the row k, we may write

$$C_{1,k}(T_{1,k-1} - T_{1,k}) = C_{2,k}(T_{2,k-1} - T_{2,k}) \tag{3}$$

where $C_{1,k}$ and $C_{2,k}$ are the hot and cold gas heat capacity rates. Substituting Equations 2 and 3 into Equation 1, this becomes

$$\varepsilon_k = \frac{\omega_{1,k}\,\omega_{2,k}}{\omega_{1,k} + C_k^* \omega_{2,k}} \tag{4}$$

where $C_k^* = C_{2,k}/C_{1,k}$ is the ratio of the hot to cold gas heat capacity rate. For $C_k^* \le 1$, ε_k is the thermal effectiveness as defined by Kay and London (1965). The hot and cold side effectiveness $\omega_{j,k}$ may be expressed, as suggested by Kay and London (1965), as a function of the heat transfer characteristics

$$\omega_{j,k} = 1 - e^{-(U_{j,k} A_j / C_{j,k})} \tag{5}$$

where $U_{j,k}$ is the overall heat transfer coefficient for side j of row k

$$U_{j,k} = \left[\frac{A_j}{(A_{0_j} + A_{F_j} E_{j,k})\, h_{out_{j,k}}} + \frac{\delta_P}{K_P} + \frac{1}{h_{in_{j,k}}} \right]^{-1} \tag{6}$$

where A_j is the total surface area, A_{F_j} the finned surface area, $A_{0_j} = (A_j - A_{F_j})$ the unfinned pipe surface area, $E_{j,k}$ the fin efficiency defined in Appendix A, δ_P the tube wall thickness, K_P the tube wall thermal conductivity, $h_{out_{j,k}}$ the average heat transfer coefficient between gas-stream and thermosyphons, $h_{in_{j,k}}$ the average heat transfer coefficient inside the evaporator (j = 1) or condenser (j = 2) of heat pipes.

The convection heat transfer coefficient $h_{out_{j,k}}$ from or to the gas in cross flow over the heat pipes, may be well approximated by the correlations proposed by Zhukauskas (1980) for in-line and staggered configuration, respectively,

$$Nu_{j,k} = 0.266\, c_k^{-0.375} Re_{j,k}^{0.625}$$

$$5000 \le Re_{j,k} \le 100{,}000 \quad \text{(in line)} \tag{7'}$$

$$Nu_{j,k} = C\, c_k (A_j^*)^n \left[\frac{a}{b}\right]^p \left[\frac{s}{D}\right]^q \left[\frac{h_F}{D}\right]^r Re_{j,k}^{\,m}$$

$$Re_{j,k} \ge 20 \quad \text{(staggered)} \tag{7"}$$

where all properties are evaluated, as reported by Zhukauskas

(1980), at the row inlet temperature; C, n, p, q, r and m are listed in Table 1; c_k is a function of tube row position in the bank, shown in Figure 1; $A_j^* = A_j / A_{P_j}$ the ratio of total surface area to heat-pipe evaporator (j = 1) or condenser (j = 2) surface area; a the transverse pitch (interaxis distance between tubes in a row); b the longitudinal pitch (distance between rows); s the distance between the fins; h_F the fin height (for plate fin, $h_F = \sqrt{ab/\pi} - D/2$ as proposed by Zhukauskas, 1980); D the tube outer diameter; D is also used as characteristic length in the Reynolds and Nusselt numbers; finally, the gas average velocity in the throat section (minimum area section) between two tubes in a row is used as characteristic velocity in the Reynolds number.

If the heat pipes are closed two-phase thermosyphons, the heat transfer coefficient $h_{in_{j,k}}$ inside the evaporator (j = 1) and condenser (j = 2), may be well approximated by the correlations proposed by Niro et al. (1990)

$$h_{in_{1,k}} = 55\, M_m^{-0.5}\, p_{r_k}^{0.12}\, (-\mathrm{Log}\, p_{r_k})^{-0.55}\, (\pi\, D L_1)^{-0.67}\, \dot{q}_{P_k}^{0.67} \qquad (8')$$

$$h_{in_{2,k}} = c \left[\frac{\pi D \rho_f (\rho_f - \rho_g)\, g\, h_{fg}\, k_f^3}{4 \mu_f} \right]^{0.33} \dot{q}_{P_k}^{-0.33} \qquad (8'')$$

where M_m is the molar mass of the working fluid charged into thermosyphons; $p_{r_k} = p_{g_k} / p_{cr}$ the operating pressure, expressed as reduced pressure, that may be assumed equal to the saturation pressure corresponding to T_{g_k}; L_1 the evaporator length; $\dot{q}_{P_k}$ the heat transfer rate per thermosyphon; c a constant equal to 1 for water and 1.5 for the other fluids. Equation 8', which has been also proposed by Groß (1990), holds for thermosyphons operating in the fully-developed boiling regime, i.e., the regime which yields optimal operations as discussed by Niro and Beretta (1990).

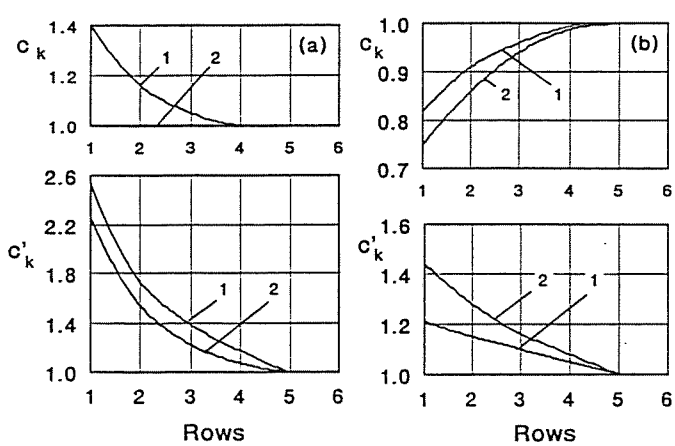

FIG. 1. Coefficients c_k and c_k' in Equations 7" and 14", respectively, for (a) in-line configuration and (b) staggered configuration (line 1 for Re = 1200, and line 2 for Re = 50 000). From Zhukauskas (1980).

Table 1. Coefficients in Equation 7"

Re range	C	n	p	q	r	m
20 ≤ Re ≤ 500	0.245	0	0	0	0	0.580
500 ≤ Re ≤ 10000	0.400	-0.375	0	0	0	0.625
10000 ≤ Re ≤ 200000	0.043	0	0.2	0.18	-0.14	0.800
200000 ≤ Re	0.007	0	0.2	0.18	-0.14	0.950

The hot and cold gas inlet temperatures to tube-row k, as derived in Appendix B, are respectively

$$T_{1,k} = T_{1,0} - (T_{1,0} - T_{2,N})(1 - \bar{C}^*) \times \times \left[\sum_{i=0}^{k-1} (C_{i+1}^* \Phi_{i+1} \prod_{j=0}^{i} \Psi_j) \right] \left[(\prod_{i=0}^{N} \Psi_i) - \bar{C}^* \right]^{-1} \qquad (9)$$

$$T_{2,k} = T_{2,N} + (T_{1,0} - T_{2,N}) \times \times \left[\prod_{i=0}^{N} (\Psi_i) - 1 - (1 - \bar{C}^*) \sum_{i=0}^{k-1} (\Phi_{i+1} \prod_{j=0}^{i} \Psi_j) \right] \left[\prod_{i=0}^{N} (\Psi_i) - \bar{C}^* \right]^{-1} \qquad (10)$$

where $\Phi_i = \varepsilon_i / (1 - \varepsilon_i)$, $\Psi_i = (1 - C_i^* \varepsilon_i)/(1 - \varepsilon_i)$ and $\bar{C}^*$ are functions defined in Appendix B, $T_{1,0}$ and $T_{2,N}$ are the inlet temperatures to the heat exchanger of the hot and cold gas respectively, and N the number of tube-rows in the exchanger. Equations 9 and 10 give the inlet temperatures to a tube-row as a function of the inlet temperatures $T_{1,0}$ and $T_{2,N}$ (known) to the exchanger, and row-effectiveness ε_k (unknown).

Solving Equations 2 and 3 for T_{g_k} we obtain

$$T_{g_k} = \frac{\omega_{1,k} T_{1,k-1} + C_k^* \omega_{2,k} T_{2,k}}{\omega_{1,k} + C_k^* \omega_{2,k}} \qquad (11)$$

i.e., the thermosyphon operating temperature expressed as a function of the hot and cold side effectiveness and the inlet temperatures to the tube-row. In addition, the heat transfer rate per thermosyphon is

$$\dot{q}_{P_k} = C_{1,k} (T_{1,k-1} - T_{1,k}) / M \qquad (12)$$

where M is the number of thermosyphons per row. Obviously,

the operating temperature and pressure of each thermosyphon and the power throughput must satisfy the conditions for the onset of the fully-developed boiling regime, as well as the limits to the heat transport.

The overall pressure drop across the heat exchanger is

$$\Delta P_j = \sum_{k=1}^{N} \Delta p_{j,k} \qquad (13)$$

where $\Delta p_{j,k}$ is the pressure drop through the tube row k, that may be approximated by the correlations proposed by Zhukauskas (1980) for in-line and staggered configuration respectively

$$Eu_{j,k} = 0.068\, c_k' A^{*0.5} \left[\frac{a^* - 1}{b^* - 1}\right]^{-0.4}$$

$$1000 \le Re_{j,k} \le 100{,}000 \quad \text{(in line)} \quad (14')$$

$$Eu_{j,k} = C'\, c_k' \left[\frac{A^*}{a^{*1.1}\, b^*}\right]^{0.5} Re_{j,k}^{\,m'}$$

$$Re_{j,k} \ge 20 \quad \text{(staggered)} \quad (14'')$$

where all properties are evaluated at the inlet temperature to the row; Eu is the Euler number (using as characteristic velocity the gas average speed in the throat section between two tubes); C' and m' are listed in Table 2, c_k' is a function of the row position in the bank, shown in Figure 1; $a^* = a/D$ and $b^* = b/D$ are the dimensionless transverse and longitudinal pitch, respectively.

For prescribed mass flowrates and inlet gas temperatures to the heat exchanger, and geometric characteristics, solving Equations 4 - 14 we can evaluate the hot and cold gas outlet temperatures from each row, the overall effectiveness and the pressure drops across the exchanger. Obviously, Equations 4 - 14 must be solved iteratively. For example, the iteration process we adopted starts with a guess for the hot and cold gas inlet temperatures $T^0_{j,k}$ to each row, and for the operating temperatures $T^0_{g_k}$ of the thermosyphons. Using the valuues of the inlet temperatures, Equations 4-8 and 12 may be solved in cascade in reverse order. Naturally, thermophysical gas properties must be evaluated at each node. Once the values of row effectiveness ε_k are calculated, a new guess of the temperatures $T^1_{j,k}$ and $T^1_{g_k}$ may be found by means of the Equations 9 - 11. The process is iterated until convergence is achieved. Knowing all the inlet temperatures and row-effectivenesses, we can finally evaluate the heat transfer rate from the hot to the cold gas streams through each tube-row, the overall heat transfer rate in the exchanger, the overall effectiveness (Equation B.11) and the pressure drop across the exchanger (Equations 13 and 14).

Table 2. Coefficients in Equations 14"

Re range	C'	m'
$20 \le Re \le 1000$	67.6	-0.69
$1000 \le Re \le 100000$	3.2	-0.25
$100000 \le Re$	0.18	0

NUMERICAL RESULTS AND DISCUSSION

We discuss the thermal performances of a heat pipe-heat exchanger using closed two-phase thermosyphons with plate fins. The numerical results concern a case of practical interest, i.e., the waste heat recovery from air at relatively low temperature to heat a supply of air at environment temperature. Thermosyphons are made of copper tubes of 15 mm o.d., 0.5 mm wall thickness, and 1000 mm long with evaporator and condenser of equal length (500 mm). The fins are made of aluminium sheets of 0.25 mm thickness, with 2.5 mm spacing. The thermosyphons are placed in a staggered configuration with 30 mm transverse pitch, and 40 mm longitudinal pitch. The heat transfer surface area density of this exchanger, therefore, is approximately 650 m^2/m^3.

The hot and cold air inlet temperatures are 200 °C and 20 °C respectively, and the outlet pressure of each stream from the

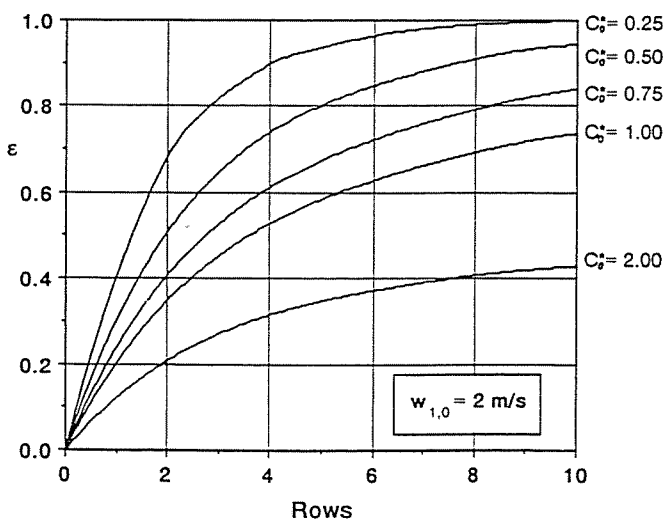

FIG. 2. Exchanger effectiveness vs. row numbers for C_0^* from 0.25 to 2 and $w_{1,0} = 2$ m/s.

exchanger is atmospheric. The thermosyphons use water as the working fluid. The number N of tube-rows is assumed in the range between 2 and 10, the hot air inlet velocity $w_{1,0}$ between 1 and 5 m/s, and the inlet heat capacity ratio C_0^* between 0.25 and 2. Finally, the thermophysical properties of air are evaluated by interpolation formulas with errors less than 1%.

Figure 2 shows the trend of the exchanger effectiveness ε as a function of N, for values of C_0^* from 0.25 to 2 and for $w_{1,0} = 2$ m/s. Obviously, the effectiveness increases as the row number increases and as the heat capacity ratio decreases. For $C^* \leq 1$, the effectiveness is the thermal effectiveness.

Figure 3 shows ε plotted against N, for values of $w_{1,0}$ from 1 to 5 m/s and for $C_0^* = 1$. As espected, for a given number of rows the exchanger effectiveness decreases as the hot gas inlet velocity increases. Indeed, the heat transfer coefficient, between gas stream and thermosyphons is proportional to $w^{0.6} \cdot w^{0.95}$ (Equations 7), but each ratio $U_{j,k}/C_{j,k}$, is proportional to $w^{-0.4} \cdot \cdot w^{-0.05}$ so that the heat pipe side effectiveness $\omega_{j,k}$ (Equation 5) is roughly proportional to $w^{-0.3}$. Consequently, the row effectiveness and, therefore, the exchanger effectiveness decrease as the gas inlet velocity increases. Finally, the exchanger effectiveness increases for increasing values of the longitudinal pitch, and for decreasing values of the transverse pitch and fin spacing.

Figure 4 shows the trend of the total rate of heat transfer per unit area of frontal surface as a function of $w_{1,0}$, for values of N from 2 to 10 and for $C_0^* = 1$. As can be seen from the figure, the total rate of heat transfer between hot and cold gases increases

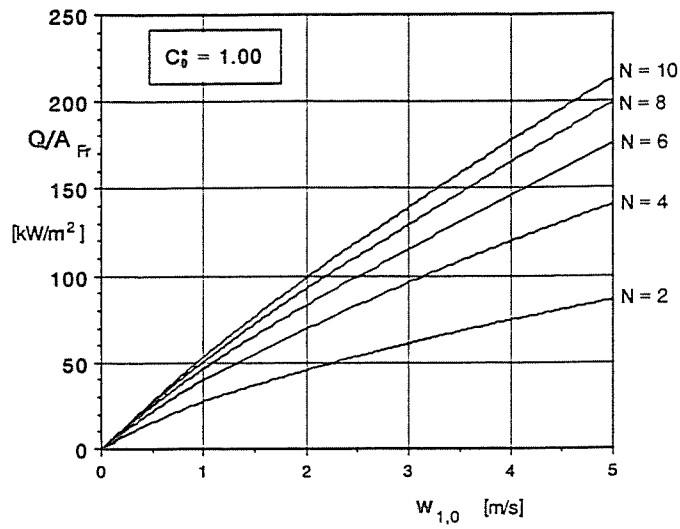

FIG. 4. Total heat transfer rate per unit frontal surface area vs. hot gas inlet velocity for row numbers from 2 to 10 and $C_0^* = 1$.

with velocity w and number of rows N. This result is not inconsistent with the effectiveness decrement for increasing values of w discussed above. In fact, the total rate of heat transfer is

$$\dot{Q} \approx C_{1,0}\, C_0^*\, \varepsilon\, (T_{1,0} - T_{2,N})$$

where $C_{1,0}$ is proportional to w, whereas ε is proportional to $w^{-0.3}$; thus, $\dot{Q} \approx w^{0.85}$, i.e., it increases as w increases.

Figures 5 and 6 show the trend of pressure drops for the hot

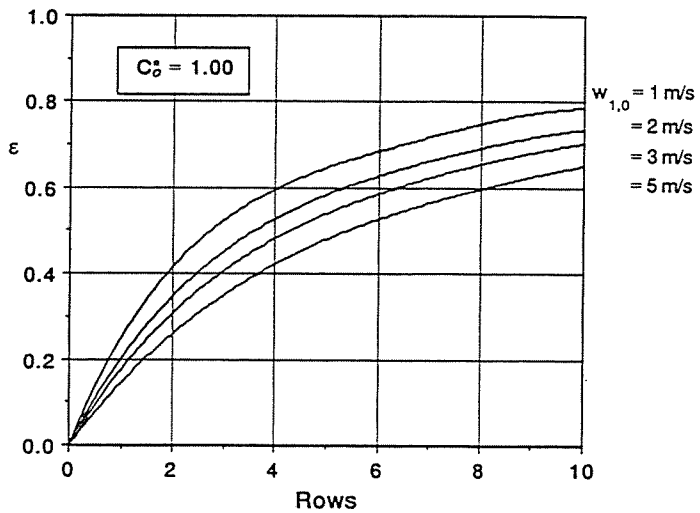

FIG. 3. Exchanger effectiveness vs. row numbers for $w_{1,0}$ from 1 to 5m/s and $C_0^* = 1$.

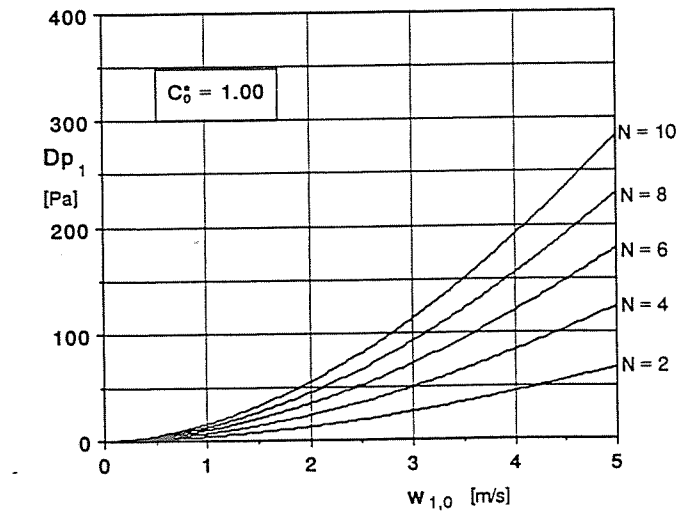

FIG. 5. Hot stream pressure drop vs. inlet velocity for row numbers from 2 to 10.

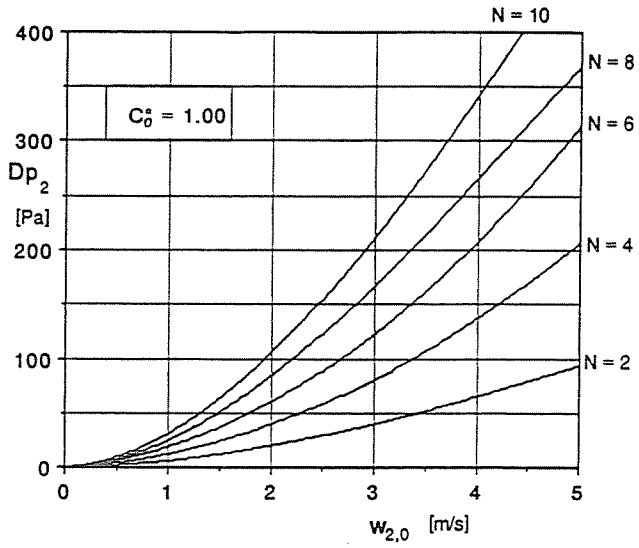

FIG. 6 Cold stream pressure drop vs. inlet velocity for row numbers from 2 to 10.

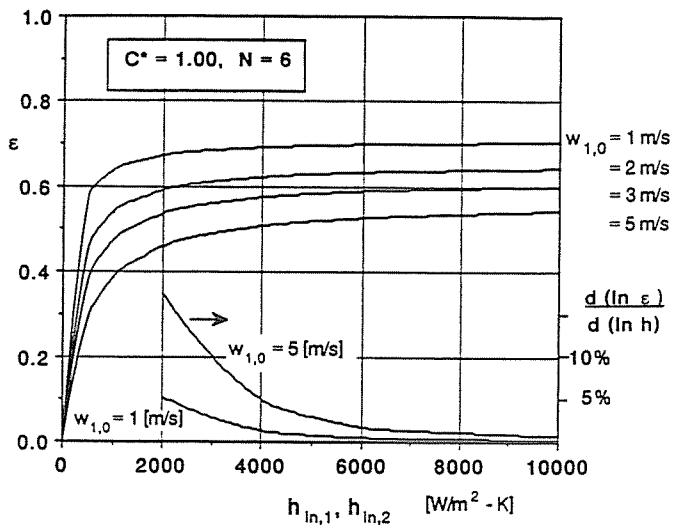

FIG. 7 Exchanger effectiveness vs. heat transfer coefficients inside the thermosyphons for $w_{1,0}$ from 1 to 5m/s, N = 6 and $C_0^* = 1$.

and cold gas streams respectively, as a function of the corresponding inlet velocity, for values of N from 2 to 10 and for $C_0^* = 1$. Obviously, pressure drop increases for increasing values of the inlet velocity and the number of rows, and for decreasing values of both longitudinal and transverse pitch, and fin spacing. Figures 5 and 6 show that, for a given inlet velocity, the pressure drop for the cold gas stream is larger, up to 60%, than that for the hot gas stream. However, for $L_1 \approx L_2$ and for $C_0^* \leq 1$, the cold gas inlet velocity is smaller than $w_{1,0}$ and, therefore, the pressure drop becomes almost the same for both streams.

Finally, Figure 7 shows ε plotted against the heat transfer coefficient inside the thermosyphons. For the purposes of this figure only, the values of h_{in_1} and h_{in_2} are assumed equal, and ε is computed for values of $w_{1,0}$ from 1 to 5 m/s, and for N = 6 and $C_0^* = 1$. The Figure shows that the exchanger effectiveness is an increasing function of h_{in_j} but the effect is important only for values of h_{in_j} up to 4000 W/m^2, whereas it is quite moderate for h_{in_j} larger than 5000 W/m^2. In fact, the logarithmic increment of ε, also plotted in Figure 7, becomes less than 5% for $h_{in} \geq 4000$ W/m^2. Consequently, if the inside boiling and condensation heat transfer coefficents have values higher than about 4000 W/m^2 (if water is the working fluid), then any increase in their values brings about a very little improvement in the exchanger performance. In other words, the thermal resistances inside the thermosyphons become negligible for relatively low values of boiling and condensation heat transfer coefficients. This extra heat transfer capability of thermosyphons represents a margin of safety in the design of a thermosyphon heat exchanger.

SUMMARY AND COCLUSIONS

We have presented an analytical model to evaluate the thermal performance and the pressure drops of a thermosyphon heat exchanger. We have reviewed the correlations to estimate the heat transfer coefficients both inside and outside thermosyphons, and the gas pressure drops through the exchanger. We have derived an analytical correlation to evaluate the gas inlet temperatures to a tube-row as a function of row effectivenesses and heat capacity rates. We have correlated the row effectiveness to the exchanger effectiveness. Finally, we have analyzed numerically the performances of a thermosyphon heat exchanger as predicted by the model for a low-temperature waste-heat application. Further refinement of the model requires experimental validation.

ACKNOWLEDGMENTS

This work was supported by MURST, the Italian Ministero dell'Università e della Ricerca Scientifica e Tecnologica.

REFERENCES

Groß, U., 1990, "Pool boiling heat transfer inside a two-phase thermosyphon. Correlation of experimental data," *Proceedings, 9th International Heat Transfer Conference*, G. Hetsroni et al., ed., Hemisphere Publishing Corp., Washington, D.C., Vol. 1, pp. 57-62.

Huang, B. J., and Tsuei, J. T., 1985, "A method of analysis for heat pipe heat exchangers," *Int. Journal of Heat and Mass Transfer*, Vol. 28, pp. 553-562.

Kay, W. M., London, A. L., 1964, "Compact heat exchangers", McGraw-Hill Book Co., New York, 1964, pp. 264-268.

Kraus, A. D., 1982 "Extended surface thermal systems", Hemisphere Publishing Corp., Washington, D.C., pp. 141-152.

Lee, Y., Bedrossian, A., 1978, "The characteristics of heat exchangers using heat pipes or thermosyphons," *Int. Journal of Heat and Mass Transfer*, Vol. 21, pp. 221-228.

Niro, A., Beretta, G. P., 1990, "Boiling Regimes in a closed two-phase thermosyphon". *Int. Journal of Heat and Mass Transfer*, Vol. 33, pp. 2099-2110.

Niro, A., Radaelli, G., Andreini, P. A., 1990, "Heat transfer characteristics in a closed two-phase thermosyphon," *Proceedings, 9th International Heat Transfer Conference*, G. Hetsroni et al., ed., Hemisphere Publishing Corp., Washington, D.C., Vol. 2, pp. 81-86.

Zhukauskas, A., 1980, "Air-cooled heat exchangers," Heat exchangers: thermal-hydraulic fundamentals and design, S. Kakac, A. E. Bergles and F. Mayinger, ed., Hemisphere Publ. Corp., New York, 1980, pp. 73-81.

APPENDIX A

The efficiency of an annular fin of rectangular profile and uniform cross-sectional area, from its definition (ratio of the fin heat transfer rate to the heat transfer rate that would exist if the entire fin surface were at the base temperature), is

$$E = \frac{2R_0}{R_e^2 - R_0^2}\left[\frac{I_1(mR_e)K_1(mR_0) - K_1(mR_e)I_1(mR_0)}{I_0(mR_0)K_1(mR_e) - I_1(mR_e)K_0(mR_0)}\right] \qquad (A.1)$$

where R_0 and R_e are, respectively, the internal and external radii of the fin; m is equal to $\sqrt{2h_{ext}/K_F\delta_F}$ with δ_F the fin thickness; I_0, I_1, K_0 and K_1 are the modified Bessel functions reported by Kraus (1982). For a plate fin, we assume that the external radius is given by the equivalent radius $R_{eq} = \sqrt{ab/\pi}$.

APPENDIX B

From Equations 1 and 3 we obtain

$$T_{1,k-1} - T_{1,k} = C_k^* \Phi_k (T_{1,k-1} - T_{2,k-1}) \qquad (B.1')$$

$$T_{2,k-1} - T_{2,k} = \Phi_k (T_{1,k-1} - T_{2,k-1}) \qquad (B.1'')$$

where $\Phi_k = \varepsilon_k/(1 - \varepsilon_k)$. Equations B.1 give the temperatures at the node k as a function of temperatures at the node k-1. Subtracting Equation B.1" from Equation B.1' and rearranging the terms, we obtain

$$\frac{T_{1,k} - T_{2,k}}{T_{1,k-1} - T_{2,k-1}} = \Psi_k \qquad (B.2)$$

where $\Psi_k = (1 - C_k^* \varepsilon_k)/(1 - \varepsilon_k)$. Since we may write

$$\frac{T_{1,k-1} - T_{2,k-1}}{T_{1,0} - T_{2,0}} = \prod_{i=1}^{k-1} \frac{T_{1,i} - T_{2,i}}{T_{1,i-1} - T_{2,i-1}} \qquad (B.3)$$

substituting Equation B.2 into Equation B.3, this becomes

$$\frac{T_{1,k-1} - T_{2,k-1}}{T_{1,0} - T_{2,0}} = \prod_{i=0}^{k-1} \Psi_i \qquad (B.4)$$

provided that $\Psi_0 \equiv 1$, i.e., $\varepsilon_0 \equiv 0$. Substituting Equation B.4 into Equations B.1, these become

$$T_{1,k-1} - T_{1,k} = C_k^* \Phi_k \left[\prod_{i=0}^{k-1} \Psi_i\right](T_{1,0} - T_{2,0}) \qquad (B.5')$$

$$T_{2,k-1} - T_{2,k} = \Phi_k \left[\prod_{i=0}^{k-1} \Psi_i\right](T_{1,0} - T_{2,0}) \qquad (B.5'')$$

Since we may write

$$T_{j,0} - T_{j,k} = \sum_{i=0}^{k-1} (T_{j,i} - T_{j,i-1}) \qquad (B.6)$$

substituting Equations B.5 into Equation B.6, we find the following relations

$$T_{1,0} - T_{1,k} = \left[\sum_{i=0}^{k-1} \left(C_{i+1}^* \Phi_{i+1} \prod_{j=0}^{i} \Psi_j\right)\right](T_{1,0} - T_{2,0}) \qquad (B.7')$$

$$T_{2,0} - T_{2,k} = \left[\sum_{i=0}^{k-1} \left(\Phi_{i+1} \prod_{j=0}^{i} \Psi_j\right)\right](T_{1,0} - T_{2,0}) \qquad (B.7'')$$

that give the temperatures at the node k as a function of $T_{1,0}$ (known) and $T_{2,0}$ (unknown). If we define the exchanger effectiveness

$$\varepsilon = \frac{T_{2,0} - T_{2,N}}{T_{1,0} - T_{2,N}} \qquad (B.8)$$

where $T_{1,0}$ and $T_{2,N}$ are, respectively, the hot and cold gas inlet temperatures to the exchanger (known), and $T_{2,0}$ the cold gas outlet temperature from the exchanger (unknown). Solving Equation B.8 for $T_{2,0}$ and sustituting into Equations B.7, we obtain

$$T_{1,k} = T_{1,0} - (1-\varepsilon)\left[\sum_{i=0}^{k-1}\left(C^{*}_{i+1}\,\Phi_{i+1}\prod_{j=0}^{i}\Psi_j\right)\right](T_{1,0} - T_{2,N}) \qquad (B.9')$$

$$T_{2,k} = T_{2,N} + \left[\varepsilon - (1-\varepsilon)\sum_{i=0}^{k-1}\left(\Phi_{i+1}\prod_{j=0}^{i}\Psi_j\right)\right](T_{1,0} - T_{2,N}) \qquad (B.9'')$$

If we write ε in the following form, as proposed by Kay and London (1964)

$$\varepsilon = \left[\frac{T_{1,N} - T_{2,N}}{T_{1,0} - T_{2,0}} - 1\right]\left[\frac{T_{1,N} - T_{2,N}}{T_{1,0} - T_{2,0}} - \frac{T_{1,0} - T_{2,N}}{T_{2,0} - T_{2,N}}\right]^{-1} \qquad (B.10)$$

using Equation B.3 (for k - 1=N), we find

$$\varepsilon = \left[\left(\prod_{i=0}^{N}\Psi_i\right) - 1\right]\left[\left(\prod_{i=0}^{N}\Psi_i\right) - \bar{C}^{*}\right]^{-1} \qquad (B.11)$$

where

$$\bar{C}^{*} = \frac{T_{1,0} - T_{2,N}}{T_{2,0} - T_{2,N}} =$$

$$= \left[\sum_{i=0}^{N-1}\left(C^{*}_{i+1}\,\Phi_{i+1}\prod_{j=0}^{i}\Psi_j\right)\right]\left[\sum_{i=0}^{N-1}\left(\Phi_{i+1}\prod_{j=0}^{i}\Psi_j\right)\right]^{-1} \qquad (B.12)$$

Finally, substituting Equation B.11 into Equations B.9, we obtain Equations 9 and 10. that give the gas inlet temperatures to a tube-row as a function of $T_{1,0}$ and $T_{2,N}$ (known) and ε_k (unknown).